Chaos, Solitons & Fractals 76 (2015) 72–81

Contents lists available at ScienceDirect

Chaos, Solitons & Fractals

Nonlinear Science, and Nonequilibrium and Complex Phenomena

journal homepage: www.elsevier.com/locate/chaos

Effect of bounded noise on chaotic motions of stochastically perturbed slowly varying oscillator

Zhen Chen, X.B. Liu *

State Key Lab of Mechanics and Control for Mechanical Structures, College of Aerospace Engineering, Nanjing University of Aeronautics and Astronautics, 29 Yudao Street, Nanjing 210016, PR China

ARTICLE INFO

Article history:
Received 15 October 2014
Accepted 25 February 2015

ABSTRACT

The effect of bounded noise on the chaotic behavior of a class of slowly varying oscillators is investigated. The stochastic Melnikov method is employed and then the criteria in both mean and mean-square sense are derived. The threshold amplitude of bounded noise given by stochastic Melnikov process is in good comparison with one determined by the numerical simulation of top Lyapunov exponents. The presence of noise scatters the chaotic domain in parameter space and the larger noise intensity results in a sparser and more irregular region. Both the simple cell mapping method and the generalized cell mapping method are applied to demonstrate the effects of noises on the attractors. Results show that the attractors are diffused and smeared by bounded noise and if the noise intensity increases, the diffusion is exacerbated.

1. Introduction

The research on chaotic phenomena in nonlinear dynamical systems has been engaging the attention and interest of researchers for many decades, since Lorenz [1] proposed a remarkable system representing a flow in three-dimensional space. However, it is particularly known that noise is inevitably present in the real world when one considers the dynamics of a system. In recent years, the effects of noise on nonlinear systems exhibiting chaotic behaviors have aroused considerable attention. Bulsara et al. [2] took into account the effects of weak additive noise on chaotic attractors of the rf SQUID. The effect of noise on the evolution of cooperation was mentioned in the studies of Wang et al. [3,4]. Frey and Simiu [5,6] developed the method of Melnikov, which is a technique providing necessary conditions for the occurrence of chaos in deterministic systems, to a class of single degree of freedom system with stochastic excitation. The generalized stochastic Melnikov method was employed to derive a mean–square criterion of a periodically forced Duffing system with additive Gaussian white noise by Lin and Yim [7], which leads to a conclusion that the presence of noise lowered the threshold and enlarged the possible chaotic domain in parameter space. The effects of external or parametric bounded noise on the chaotic behavior of the Duffing oscillator have been analyzed by Xu et al. [8] and Zhu et al. [9]. As an extension to high-dimensional case, a quasi-integrable Hamiltonian system with two degree-of-freedom was employed and the stochastic Melnikov process was derived when the harmonic and the bounded noise excitations were imposed on the system [10]. Moreover, some transient dynamics, such as mean first passage time through a potential barrier and mean growth rate coefficient as a function of the noise intensity, were studied in [11,12]. Nevertheless, the noise effect on three-dimensional systems draws paltry attention. Wiggins and Holmes [13] and Wiggins and Shaw [14] obtained necessary conditions for the occurrence of chaos in a class of slowly varying oscillators in which

* Corresponding author. Tel./fax: +86 025 84892106.
E-mail addresses: czkillua@gmail.com (Z. Chen), xbliu@nuaa.edu.cn (X.B. Liu).

http://dx.doi.org/10.1016/j.chaos.2015.02.024
0960-0779/

perturbations were periodic. Then Simiu [15] generalized these authors' theories for the case of quasiperiodic or stochastic perturbations. Besides acquiring necessary conditions for chaos induced by stochastic perturbations, he also estimated the lower bounds for the mean time of exit from preferred regions of phase space.

The main purpose of this paper is to investigate a specific stochastically perturbed slowly varying oscillator characterized by three-dimensional system adopting the generalized Melnikov technique and to show the effect of noise on chaotic behaviors and the attractors of the system.

An outline of this paper is as follows. In Section 2, initially we briefly introduce the system and the bounded noise. Subsequently we bring Sections 2.1 and 2.2 into a discussion of the geometry of the phase space of the unperturbed and perturbed system, describing the basic perturbation results. Standard linear analysis of fixed points is carried on in Section 3 and a derivation of the stochastic Melnikov process is demonstrated in Section 4. To verify the results of our analytical approach, simulations of the governing equations are performed in Section 5, in which various numerical methods are applied. Ultimately conclusions are given in Section 6.

2. Formulation

We consider a class of third order nonautonomous systems to model vibration of a feedback controlled buckled column subjected to additive noise. Its deterministic case was first proposed by Homes and Moon [16] and then examined by Wiggins [17]. The system is given by

$$\begin{aligned}\dot{x}_1 &= x_2\\ \dot{x}_2 &= x_1 - x_1^3 - I + \varepsilon(-\delta x_2 + \xi(t))\\ \dot{I} &= \varepsilon(\gamma x_1 - \alpha I)\\ \dot{\theta} &= \Omega\end{aligned} \tag{1}$$

where $\alpha,\ \gamma,\ \delta$ are parameters, Ω is positive and ε is small and fixed. $\xi(t)$ is a bounded noise which is a harmonic function with constant amplitude and random frequency and phases, whose mathematical expression is

$$\begin{aligned}\xi(t) &= \mu cos(\theta + \psi)\\ \psi &= \sigma B(t) + \Gamma\end{aligned} \tag{2}$$

where $\mu,\ \sigma$ are positive constants, $B(t)$ is a unit Wiener process, Γ is a random variable uniformly distributed in $[0, 2\pi)$. $\xi(t)$ is a stationary random process in wide sense with zero mean. Its covariance function and spectral density are respectively

$$\begin{aligned}C_\xi(\tau) &= \frac{\mu^2}{2}\exp\left(-\frac{\sigma^2\tau}{2}\right)cos\Omega\tau\\ S_\xi(\omega) &= \frac{(\mu\sigma)^2}{2\pi}\left(\frac{1}{4(\omega-\Omega)^2+\sigma^4}+\frac{1}{4(\omega+\Omega)^2+\sigma^4}\right)\end{aligned} \tag{3}$$

The variance of the noise is $C(0) = \mu^2/2$ which implies that the noise has finite power. It is a narrow-band process when σ is small and approaches to white noise as $\sigma \to \infty$. It can be shown that the sample functions of the noise are continuous and bounded which are required in the derivation of the Melnikov function [5].

2.1. The unperturbed system

The unperturbed system is given by

$$\begin{aligned}\dot{x}_1 &= x_2\\ \dot{x}_2 &= x_1 - x_1^3 - I\\ \dot{I} &= 0\\ \dot{\theta} &= \Omega\end{aligned} \tag{4}$$

and the (x_1, x_2) component of (4) has the form of a 1-parameter family of Hamiltonian systems with its Hamiltonian function given by

$$H(x_1, x_2; I) = \frac{x_2^2}{2} - \frac{x_1^2}{2} + \frac{x_1^4}{4} + Ix_1 \tag{5}$$

Fixed points of (x_1, x_2, I) component of (4) are given by $(x_1(I), 0, I)$, where $x_1(I)$ is a solution to the equation of

$$x_1^3 - x_1 + I = 0 \tag{6}$$

For $I \in \left(-2/3\sqrt{3}, 2/3\sqrt{3}\right)$, Eq. (6) has three solutions with the intermediate one corresponding to a hyperbolic fixed point. For $I > 2/3\sqrt{3}$ and $I < -2/3\sqrt{3}$, there exists only one solution of Eq. (6) corresponding to an elliptic fixed point and for $I = \pm 2/3\sqrt{3}$, Eq. (6) has two solutions corresponding to an elliptic fixed point and a saddle-node fixed point. Since we will only be interested in hyperbolic fixed points, we denote the interval $\left(-2/3\sqrt{3},\ 2/3\sqrt{3}\right)$ as J.

The hyperbolic fixed points of the (x_1, x_2, I) component of (4) form one-manifold denoted by

$$\gamma(I) = (\bar{x}_1(I),\ 0,\ I) \tag{7}$$

where $\bar{x}_1(I)$ is the intermediate root of Eq. (6) when $I \in J$. For each fixed I, i.e. for each fixed point there exists a pair of homoclinic orbits satisfying

$$\frac{x_2^2}{2} - \frac{x_1^2}{2} + \frac{x_1^4}{4} + Ix_1 = -\frac{1}{2}\bar{x}_1^2(I) + \frac{1}{4}\bar{x}_1^4(I) + I\bar{x}_1 \tag{8}$$

Thus, the phase space of (4) is shown in Fig. 1.

Therefore in the full context of (x_1, x_2, I, θ) phase space the unperturbed system (4) has a two-dimensional normally hyperbolic invariant manifold with boundary

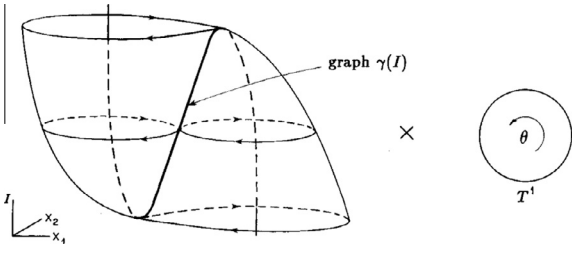

Fig. 1. Phase space of the unperturbed system (4).

$$\mathcal{M} = (\gamma(I), \theta_0), I \in J, \theta_0 \in [0, 2\pi) \tag{9}$$

and $\mathcal{M}$ has three-dimensional stable and unstable manifold which coincide. Here we would like to argue that $\mathcal{M}$ is an invariant manifold in a very unstable sense due to the fact that it is a manifold with boundary, yet it is still invariant since $\dot{I} = 0$, and therefore no orbit can cross the boundary.

2.2. The perturbed system

Next we shall turn to the perturbed system (1). According to Simiu [15], there exists ε_0 such that for $0 < \varepsilon < \varepsilon_0 \ll 1$, $\mathcal{M}$ persists as a locally invariant manifold, denoted by

$$\mathcal{M}_\varepsilon = (\gamma(I) + \mathcal{O}(\varepsilon), \theta_0), \quad I \in J, \quad \theta_0 \in [0, 2\pi) \tag{10}$$

which has both local stable and unstable manifolds. Whereas, in the perturbed system $\dot{I} \neq 0$, implying the possibility that there is no recurrent motion on $\mathcal{M}_\varepsilon$ and all points may eventually leave $\mathcal{M}_\varepsilon$ by crossing its boundary. Given that there could be dramatic dynamical consequences associated with orbits homoclinic to fixed points, periodic orbits, or normally hyperbolic tori, it is our current task to determine whether $\mathcal{M}_\varepsilon$ contains any periodic orbit and ascertain whether the stable and unstable manifolds of the periodic orbit will intersect or not by calculating appropriate Melnikov function.

Primarily let us give a thought to the vector filed (1) restricted to $\mathcal{M}_\varepsilon$, given by

$$\begin{aligned} \dot{I} &= \varepsilon[\gamma x_1(I) - \alpha I] \\ \dot{\theta} &= \Omega \end{aligned} \tag{11}$$

where $x_1(I)$ is the solution of Eq. (6). To ensure that trajectories approach the same location in forward and backward time, let $\bar{I} \in J$ be a hyperbolic fixed point for the first equation of Eq. (11), which satisfies

$$I = \frac{\gamma}{\alpha} x_1 \tag{12}$$

Note: if necessary, we may average the first equation of Eq. (11) over θ to determine $\bar{I}$. Substituting Eq. (12) into Eq. (6) gives the following expression of hyperbolic fixed points:

$$\bar{I} = 0, \quad \pm\frac{\gamma}{\alpha}\sqrt{1 - \frac{\gamma}{\alpha}} \tag{13}$$

For $\frac{\gamma}{\alpha} < 1$, the first equation of (11) has three fixed points and for $\frac{\gamma}{\alpha} > 1$ it has only one fixed point. Denote the one-dimensional periodic orbit by

$$\tau_\varepsilon(\bar{I}) = \{\, (\gamma(I), \theta) | I = \bar{I},\ \theta \in T^1 \,\} \subseteq \mathcal{M}_\varepsilon \tag{14}$$

The point $(x_1, x_2, I) = (0, 0, 0)$ is hyperbolic for all γ and α. It follows that the corresponding persistent torus and homoclinic orbits are $\tau_\varepsilon(0) = (0, 0, 0, T^1)$ and $x^0_\pm(t) = \left(\pm\sqrt{2}sech(t)\ ,\ \mp\sqrt{2}sech(t)tanh(t)\right)$. In addition, for $\bar{I} = \pm\frac{\gamma}{\alpha}\sqrt{1 - \frac{\gamma}{\alpha}}$, the other two torus are $\tau_\varepsilon\left(\pm\frac{\gamma}{\alpha}\sqrt{1 - \frac{\gamma}{\alpha}}\right) = \left(\pm\sqrt{1 - \frac{\gamma}{\alpha}},\ 0,\ \pm\frac{\gamma}{\alpha}\sqrt{1 - \frac{\gamma}{\alpha}},\ T^1\right)$.

3. Linear analysis

In this section we will focus on the stability of these fixed points of the perturbed system via linear analysis. The linearized matrix of the system (1) is the following

$$\begin{bmatrix} 0 & 1 & 0 \\ 1 - 3x_1^2 & -\varepsilon\delta & -1 \\ \varepsilon\gamma & 0 & -\varepsilon\alpha \end{bmatrix} \tag{15}$$

and suppose its eigenvalues have the form of $\lambda = \lambda_0 + \varepsilon\lambda_1 + \cdots$. Calculating the eigenvalues to the order ε leads to the following results:

For $(0, 0, 0)$

$$\lambda_I = \varepsilon(\gamma - \alpha), \quad \lambda_{II,III} = \pm 1 - \frac{\varepsilon}{2}(\gamma + \delta) \tag{16}$$

For $\left(\pm\sqrt{1 - \frac{\gamma}{\alpha}},\ 0,\ \pm\frac{\gamma}{\alpha}\sqrt{1 - \frac{\gamma}{\alpha}}\right)$

$$\lambda_I = \varepsilon\frac{2(\alpha - \gamma)}{\left[3\frac{\gamma}{\alpha} - 2\right]}, \quad \lambda_{II,III} = \pm\sqrt{3\frac{\gamma}{\alpha} - 2} - \varepsilon\left(\frac{\delta}{2} + \frac{\gamma}{2\left[3\frac{\gamma}{\alpha} - 2\right]}\right) \tag{17}$$

Then, we can make several conclusions:

(1) For $\gamma > \alpha$, there exists only one fixed point, $(0, 0, 0)$, which has a two-dimensional unstable manifold and a one-dimensional stable manifold.
(2) For $\gamma < \alpha$, there exists three fixed points, implying that a pitchfork bifurcation occurs at $\gamma = \alpha$. The point $(0, 0, 0)$ has a one-dimensional unstable manifold and a two-dimensional stable manifold. Furthermore,
  (2.1) for $\frac{2}{3}\alpha < \gamma < \alpha$, $\left(\pm\sqrt{1 - \frac{\gamma}{\alpha}}, 0, \pm\frac{\gamma}{\alpha}\sqrt{1 - \frac{\gamma}{\alpha}}\right)$ has 3 real eigenvalues, corresponding to a two-dimensional unstable manifold and a one-dimensional stable manifold;
  (2.2) for $\gamma < \frac{2}{3}\alpha$, $\lambda_I < 0$, $\lambda_{II,III}$ are complex conjugate and the sign of their real parts depend on λ_1 of order ε, i.e. $\gamma^* = \frac{2}{\frac{1}{\delta} + \frac{3}{2}}$.

From the above analysis, three important transition curves are drawn in Fig. 2 in which we fix $\alpha = 1$.

The curve $\gamma = 1$ consisting of critical parameter values of the pitchfork bifurcation, the curve $\gamma = 2/3$ associated with the change of the last two eigenvalues of $\left(\pm\sqrt{1 - \frac{\gamma}{\alpha}},\ 0,\ \pm\frac{\gamma}{\alpha}\sqrt{1 - \frac{\gamma}{\alpha}}\right)$ from purely real to complex conjugate (also the first eigenvalue changes sign on this curve), the curve $\gamma = \gamma^*$ denotes the passage of the complex eigenvalues from unstable to stable as γ decreases further.

4. Stochastic Melnikov process

The stochastic Melnikov process for system (1) can be obtained by using the formula given by Wiggins [17] and Simiu [15] as follows:

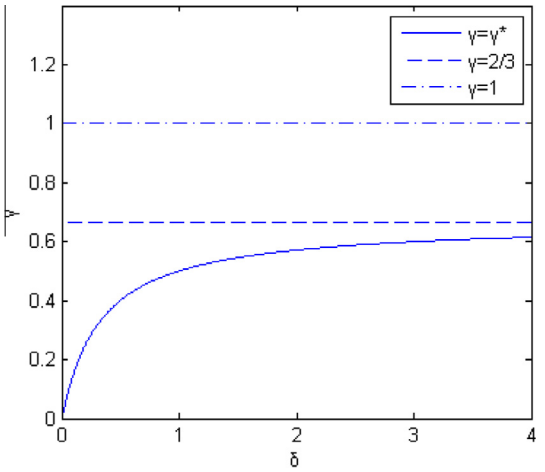

Fig. 2. Transition curves of critical eigenvalues of (15).

$$M^{\bar{I}}(t_0)=\int_{-\infty}^{+\infty}-\delta(x_2^{\bar{I}}(t))^2dt+\int_{-\infty}^{+\infty}x_2^{\bar{I}}(t)\cdot\xi(t_0-t)dt+\int_{-\infty}^{+\infty}\gamma(x_1^{\bar{I}}(t))^2dt-\alpha\int_{-\infty}^{+\infty}\bar{I}\cdot x_1^{\bar{I}}(t)\,dt-x_1(\bar{I})\cdot\int_{-\infty}^{+\infty}\gamma x_1^{\bar{I}}(t)-\alpha\bar{I}dt \tag{18}$$

where $x^{\bar{I}}(t)=(x_1^{\bar{I}}(t),x_2^{\bar{I}}(t))$ is the homoclinic orbit of the unperturbed system if $I=\bar{I}$.

For $\bar{I}=0$, $x_{\pm}^0(t)=\left(\pm\sqrt{2}sech(t),\ \mp\sqrt{2}sech(t)\cdot tanh(t)\right)$, then the integrals can be calculated by the method of residues:

$$M^0(t_0)=-\frac{4}{3}\delta+4\gamma+Z(t_0) \tag{19}$$

where $Z(t_0)=\int_{-\infty}^{+\infty}x_2^0(t)\cdot\xi(t_0-t)dt$. If we regard $h(t)=x_2^0(t)$ as the impulse response function of a time-invariant linear system and $\xi(t)$ is an input of the system, $Z(t_0)=h(t)*\xi(t)$ is the output of the system with zero mean and its variance is given by

$$\sigma_Z^2=\int_{-\infty}^{+\infty}|H(\omega)|^2\cdot S_\xi(\omega)d\omega \tag{20}$$

where $H(\omega)=\int_{-\infty}^{+\infty}h(t)\cdot e^{-j\omega t}dt=\mp j\sqrt{2}\pi\omega\mathrm{sech}(\frac{\omega\pi}{2})$ is the frequency response function.

Then we figure out the condition of the occurrence of simple zeros of stochastic Melnikov process in both mean sense

$$\gamma=\frac{1}{3}\delta \tag{21}$$

and mean-square sense

$$\left\langle-\frac{4}{3}\delta+4\gamma\right\rangle^2\leqslant\int_{-\infty}^{+\infty}\left|\sqrt{2}\,\pi\,\omega\,\mathrm{sech}\left(\frac{\pi\omega}{2}\right)\right|^2\cdot\frac{\mu^2\sigma^2}{2\pi}\cdot\left(\frac{1}{4(\omega-\Omega)^2+\sigma^4}+\frac{1}{4(\omega+\Omega)^2+\sigma^4}\right)d\omega \tag{22}$$

where $\langle\bullet\rangle$ denote the expectation operator.

By supposing $\psi=0$, system (1) degenerates to an oscillator excited by periodic perturbations, which gives the Melnikov function in deterministic sense as follows:

$$\tilde{M}^0(t_0)=-\frac{4}{3}\delta+4\gamma+\int_{-\infty}^{+\infty}x_2^0(t)\cdot\mu\cos(\Omega(t-t_0))dt \tag{23}$$

where the integral can be evaluated by using the fact that $x_2^0(t)$ is an odd function of t and the method of residues. Then we obtain

$$\tilde{M}^0(t_0)=-\frac{4}{3}\delta+4\gamma+\sqrt{2}\mu\pi\Omega\,\mathrm{sec}\,h\left(\frac{\Omega\pi}{2}\right)\cdot\sin(\Omega t_0) \tag{24}$$

Consequently the condition of the occurrence of simple zeroes of $\tilde{M}^0(t_0)$ is

$$\left|-\frac{4}{3}\delta+4\gamma\right|\leqslant\sqrt{2}\mu\Omega\,\mathrm{sec}\,h\left(\frac{\Omega\pi}{2}\right) \tag{25}$$

5. Numerical results

5.1. The top Lyapunov exponent

Lyapunov exponents are the average exponential rates of divergence or convergence of nearby orbits in phase space. Exponential divergence of nearby orbits implies sensitive dependence on initial conditions. A system with one or more positive Lyapunov exponents is usually defined to be chaotic. To verify the threshold amplitude of bounded noise for the onset of chaos in the mean-square sense obtained in Section 4, the top Lyapunov exponent of system (1) is computed by the algorithm presented by Wolf et al. [18]. Moreover, according to Eckmann [19], a stable periodic orbit has one Lyapunov exponent equal to zero and the others negative, while an attracting quasiperiodic orbit, i.e., an invariant torus T^k has k Lyapunov exponents equal to zero and the others negative.

Numerical calculations have been made by assuming the following parameters: $\Omega=1.7$, $\gamma=0.8$, $\delta=1$, $\alpha=1$, $\varepsilon=0.01$. The results of the top Lyapunov exponent versus bounded noise amplitude of system (1) are displayed in Fig. 4 and the threshold amplitude for the onset of chaos is shown in Fig. 3.

What Fig. 3 shows is that over a large range of σ value, the random Melnikov process with mean-square criterion, Eq. (22), and top Lyapunov exponents of numerical calculations yield comparable threshold amplitude μ of bounded noise. For small noise intensity σ, i.e., $\sigma<1$, the threshold μ decreases while for larger σ the threshold increases as σ increases. Due to the fact that Melnikov method only provides a necessary condition for chaos, the stochastic Melnikov process underestimates the threshold amplitude and numerical results should be larger than the analytical results. Thus it can be seen that the stochastic Melnikov process with mean-square criterion yields meaningful results for minor noise intensity.

From Fig. 4 one can see that for small values of amplitudeμ, the top Lyapunov exponent is zero, implying the motion of system is periodic. As μ increases, the top Lyapunov exponent changes from zero to positive, signifying the presence of chaotic motions. In the absence of

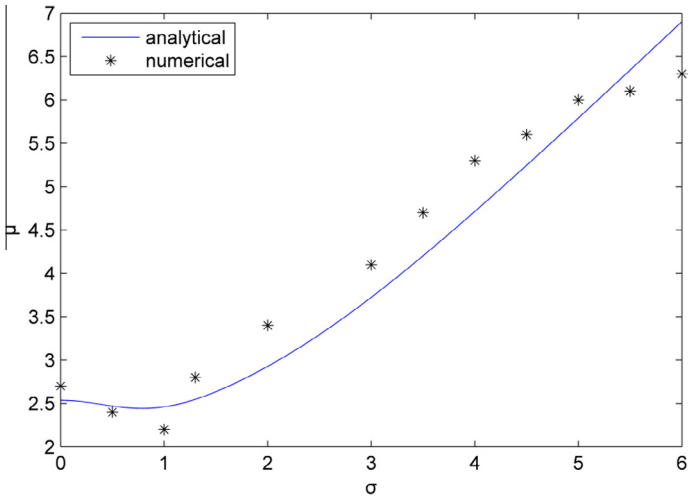

Fig. 3. The threshold amplitude of bounded noise for the onset of chaos in system (1) (∗) result by numerical calculations; (__) result by random Melnikov process, Eq. (22).

noise, i.e., $\psi = 0$ (see Fig. 4(a)), beyond the threshold $\mu = 2.7$, there are some "windows" or intervals, within which the top Lyapunov exponent becomes zero again and the system is then periodic. For larger noise intensity, no such "window" exists. Therefore one of the noise effects is to diminish or eliminate these periodic "windows" or intervals.

5.2. Effect of noise in parameter space

Standard linear analysis reveals three important transition curves in (δ, γ) parameter space shown in Fig. 2. Due to the stochastic Melnikov process, condition for the onset of chaos in the mean sense is given in Eq. (21), which is also in $\delta - \gamma$ relation. Hence Eq. (21) divides Fig. 2 into several distinguished regions displayed in Fig. 5 (a).

In Fig. 5(b)–(f), we show a series of global phase portraits of system (1) with $\psi = 0$, where the parameters pass from region I to II and from region VII to VIII. For all plots we set $\Omega = 1.7,\ \varepsilon = 0.01,\ \alpha = 1,\ \mu = 2$. These figures show steady-state motions and all transients have faded away. In passing from region I to II, the existence of an attracting limit cycle (see Fig. 5(b)) which originates outside the homoclinic orbit $x^0_{\pm}(t)$ are observed. As $\delta \to 3\gamma$, i.e., $\delta \to 3.6$, it becomes increasingly chaotic (see Fig. 5(c)) and eventually settles down to a new limit cycle (see Fig. 5(d)) which oscillates periodically from one potential well to the other. Therefore (21) does appear to be a reasonable valid predictor of chaotic motions. Furthermore, by a comparison between Fig. 5(b) and (d) a qualitative change evidently occurs in global dynamical behavior. Thus acknowledgement of (21) is crucial for understanding this transition. We note that the global dynamics behave similarly in passing from region VII to VIII (see Fig. 5(e) and (f)).

The influence of noise on the occurrence of chaotic motion in $\delta - \gamma$ parameter space is visualized in Fig. 6. For a better understanding, we also plot the $\delta - \gamma$ relations given by (25) in blue solid lines. Red points in these figures denote positive top Lyapunov exponent for current selection of δ and γ. In Fig. 6(a) we set the noise intensity $\sigma = 0$ and it can be seen that all points entirely distribute uniformly and regularly in parameter space. As the noise intensity increases (see Fig. 6(b)–(d)), their distribution exhibits a trend of sparseness and irregularity and red points undergo diffusions in the whole space except region VIII, where there exist two stable fixed points whose eigenvalues all have negative real parts. Details are given in Section 3 and see Fig. 5(f) for illustration. Also note that larger noise intensity results in more expansive distribution of red points, implying more possible chaotic domains in parameter space. In addition, for $\sigma = 4$ (see Fig. 6(d)) three "tails" emerge from the apparently irregular distribution, each of which falls into separate region, i.e., region II, IV, VI.

5.3. Attractors characterized by SCM and GCM methods

SCM (simple cell mapping) and GCM (generalized cell mapping) have been found to form a very effective tool for the global analysis of nonlinear systems and even one subjected to random excitations [20,21]. The advantage of SCM lies in its extremely efficient way which may specify the global dynamics of a system in broad strokes. On the other hand the GCM is capable of revealing a more detailed picture of the behavior pattern, but at the cost of more computational effort. Details about these two methods can be found in Hsu [22]. In this paper both methods are employed to delineate the attractor of system (1).

First of all we show in Fig. 7(a) the attractor of system (1) in the absence of noisecaptured by the method of SCM. For numerical calculations parameters are chosen as follows: $\Omega = 1.7,\ \varepsilon = 0.01,\ \alpha = 1,\ \gamma = 0.8,\ \delta = 2.4$. The parameter values are chosen so that the system shows chaotic motions without noise. The region of interest of the state space is taken to be from -1.8 to 2.0 for x_1, from -1.8 to 1.7 for x_2, and from -0.5 to 0.6 for I. 100 divisions are

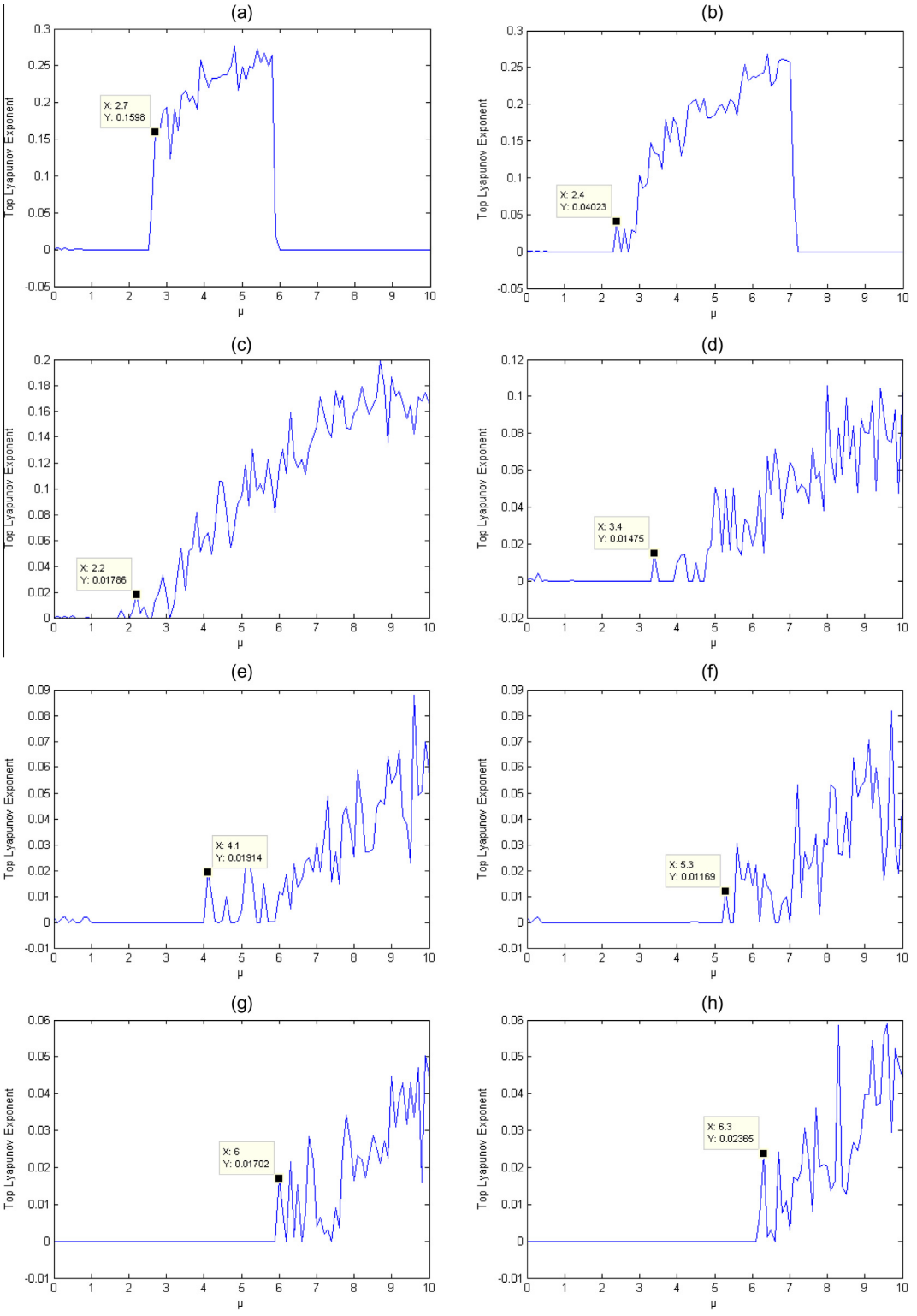

Fig. 4. The top Lyapunov exponent of system (1) (a) $\psi = 0$, (b) $\sigma = 0.5$, (c) $\sigma = 1$, (d) $\sigma = 2$, (e) $\sigma = 3$, (f) $\sigma = 4$, (g) $\sigma = 5$, (h) $\sigma = 6$.

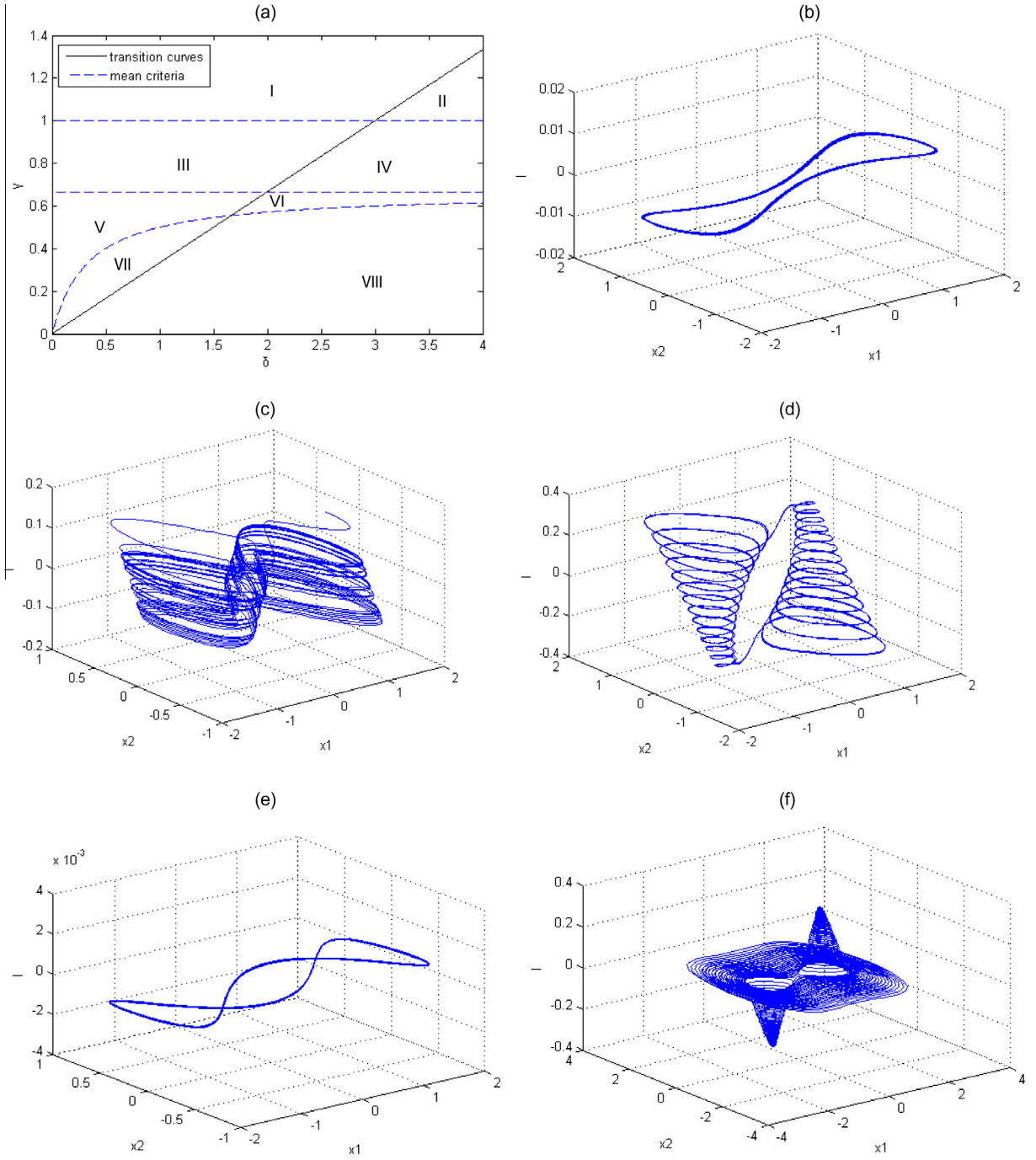

Fig. 5. (a) Distinguished regions in $\delta - \gamma$ parameter space and (b)–(f) associate steady-state phase portraits, (b) $\gamma = 1.2,\ \delta = 1$, (c) $\gamma = 1.2,\ \delta = 3.6$, (d) $\gamma = 1.2,\ \delta = 6$, (e) $\gamma = 0.3,\ \delta = 0.2$, (f) $\gamma = 0.3,\ \delta = 2$.

used for x_1 and x_2, and 50 divisions for I. Thus there are a total of 500,000 regular cells, plus a sink cell which covers the state space outside the region of interest. Centers of all periodic cells of SCM are drawn in blue points, which together constitute the attractor, as shown in Fig. 7(a). We see that it has two bulging bottoms and a link connected with each other and this just corresponds to oscillations between two fixed points (see Fig. 5(f)).

Next the bounded noise is taken into consideration and noise intensity is set to be $\sigma = 2$ and $\sigma = 5$. By similar procedure attracting cells are displayed in the following figures (see Fig. 7(b) and Fig. 8). From Fig. 7(b) it is seen

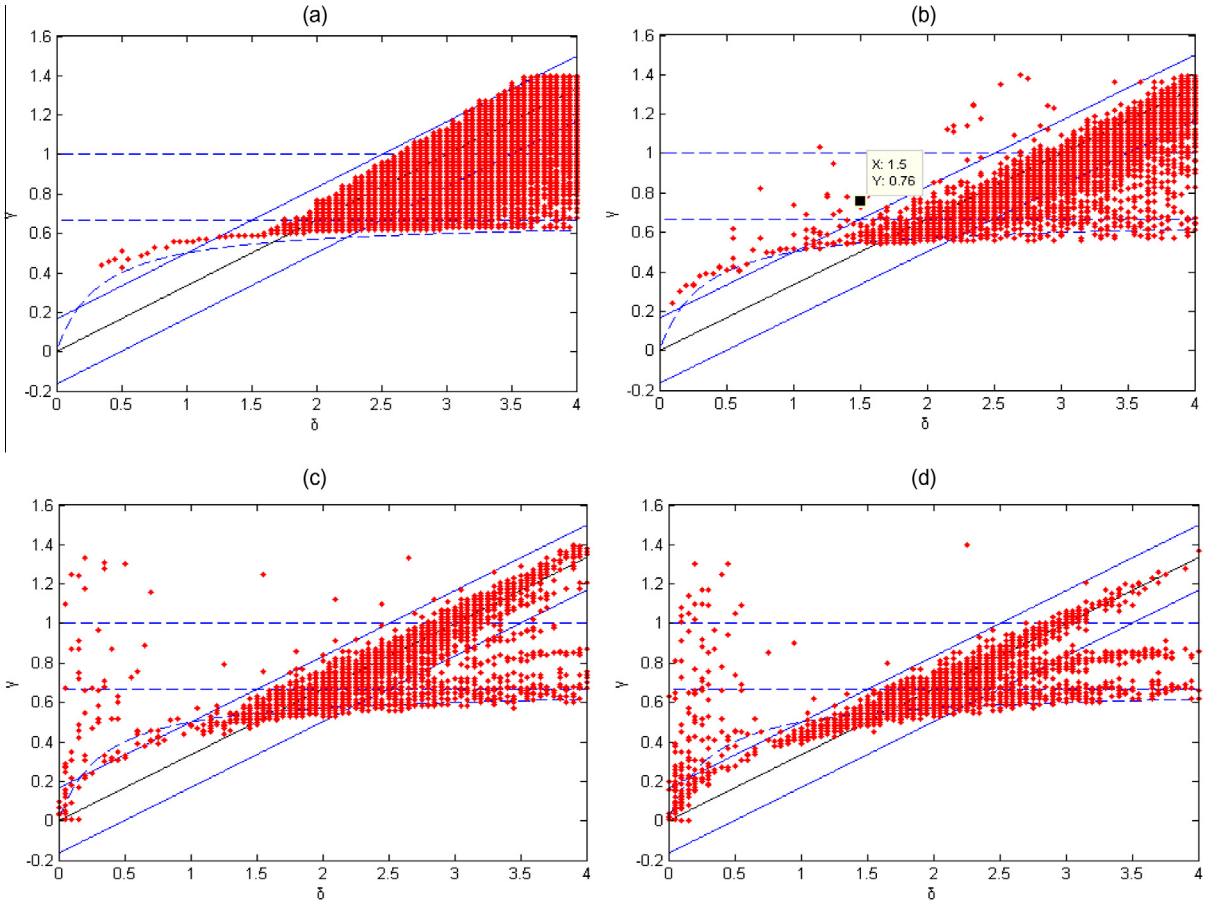

Fig. 6. Effect of noise on chaotic motions visualized in parameter space (a) $\sigma = 0$, (b) $\sigma = 1$, (c) $\sigma = 2$, (d) $\sigma = 4$.

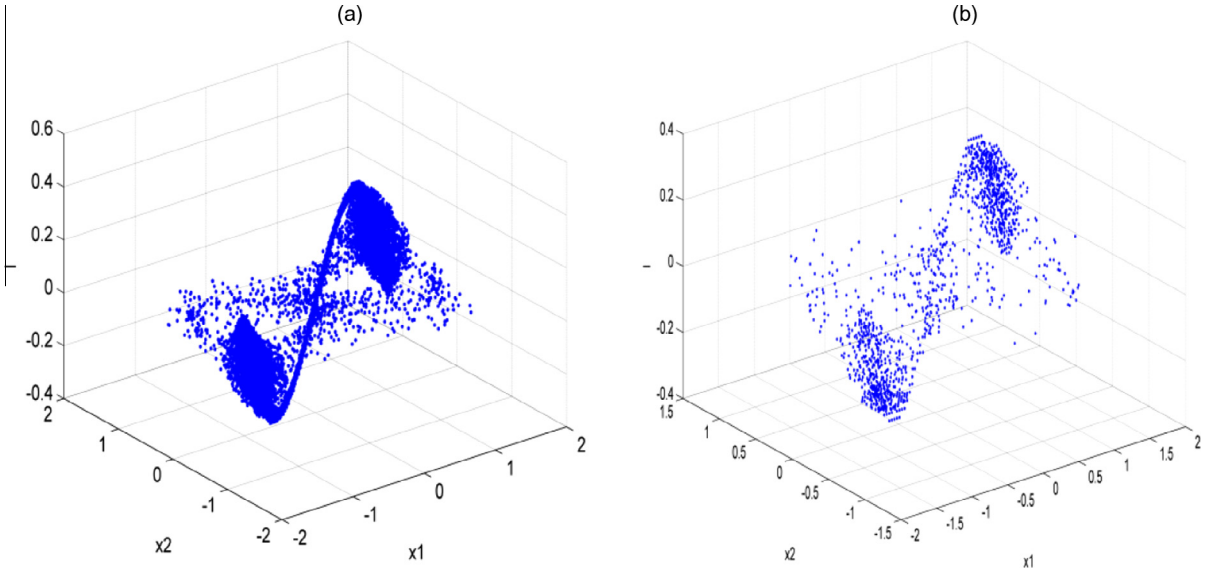

Fig. 7. Attracting cells of system (1) by SCM, (a) noise free; (b) $\sigma = 2$.

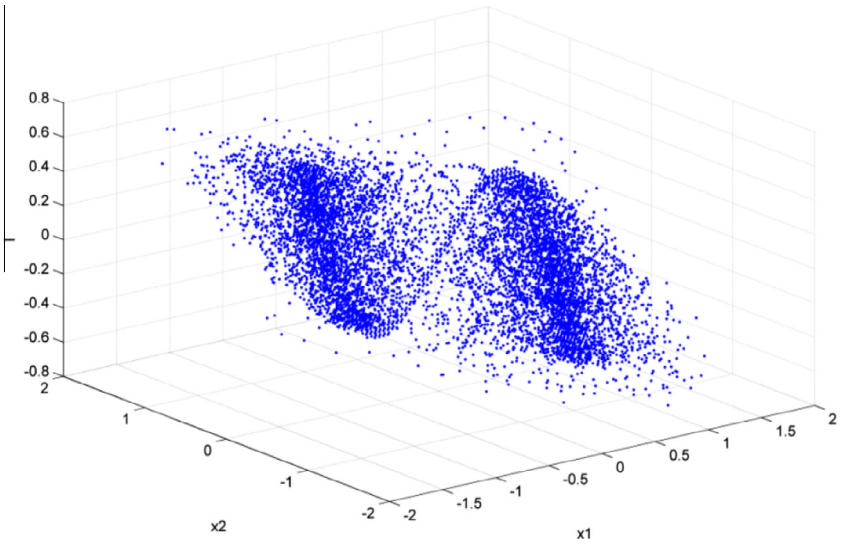

Fig. 8. Attracting cells of system (1) by SCM, $\sigma = 5$.

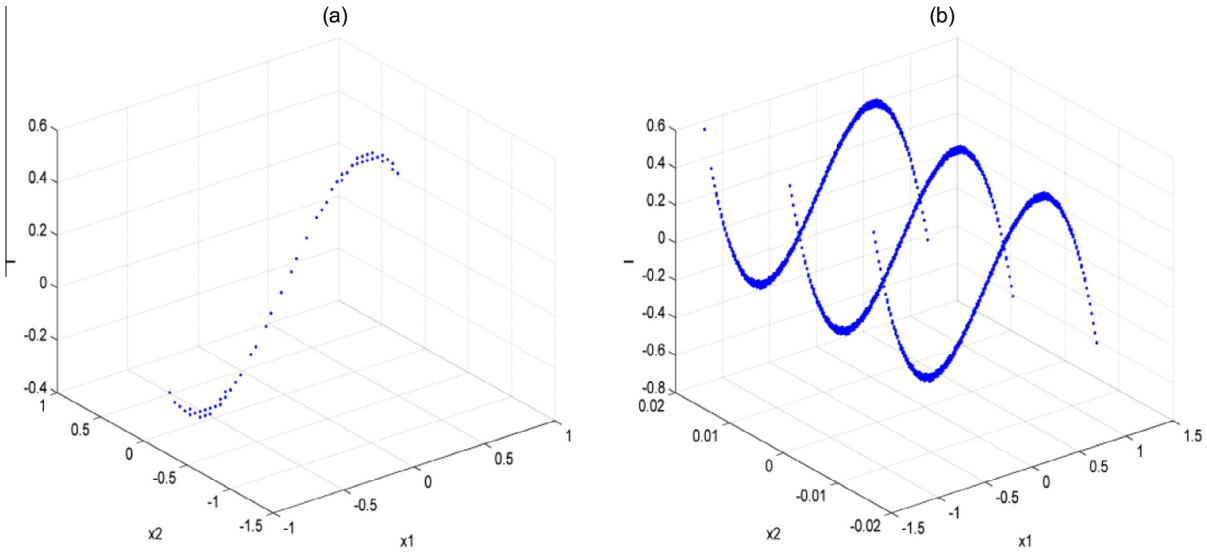

Fig. 9. Persistent group of system (1) without noise by GCM, (a) $100 \times 100 \times 50$, (b) $200 \times 200 \times 100$.

that the attractor is explicitly diffused by noise. When the noise intensity is large enough, new regions of phase space are visited due to the noise, as is shown in Fig. 8. We are convinced that it is a result of highly diffusive effect of noise.

GCM method is then implemented for further characterization of the attractor. In general a strange attractor manifests itself in GCM as a large persistent group. Depending upon whether the strange attractor is of one piece or of several pieces, the persistent group could be either acyclic or periodic. We only obtain persistent groups of GCM for system without noise, whereas for systems in the presence of noise further study is needed.

Fig. 9(a) shows the persistent group of system (1) in the absence of noise for the same cell structure as SCM, i.e., $100 \times 100 \times 50$. It can be seen that both bottoms appear to possess fine structures which is one of the geometric features of strange attractors and they exactly correspond to the bulging bottoms in Fig. 7(a) by SCM. However, if we refine the cell structure by $200 \times 200 \times 100$, the new persistent groups are then given in Fig. 9(b).

From Fig. 9(b) one can see that the attractor layers in the x_2 direction into three thin structures composed of a single thickness of cells and the distance between each piece is in order 10^{-2}, implying the existence of fine structures. Moreover, all pieces look exactly the same. For

situations with noise we believe that the fine structure will be lost.

6. Conclusions

In this paper the effect of bounded noise on chaotic motions of a class of third order systems which model the vibrations of a feedback controlled buckled column has been investigated both analytically and numerically. It is found that the stochastic Melnikov process yields comparable results with numerical calculations, which is illustrated by top Lyapunov exponents, while it is also observed that in the presence of noise the chaotic regions in parameter space becomes more and more sparse and irregular as the noise intensity increases and we can come to a conclusion that the larger noise intensity results in more possible chaotic domain in parameter space. By the methods of SCM and GCM, it can be seen bounded noise shall diffuse the attractor.

Acknowledgments

This research was supported by the National Natural Science Foundation of China (Grant Nos. 11472126 and 11232007), the Research Fund of State Key Laboratory of Mechanics and Control of Mechanical Structures (Nanjing University of Aeronautics and Astronautics) (Grant No. 0113G01) and the Project Funded by the Priority Academic Program Development of Jiangsu Higher Education Institutions (PAPD).

References

[1] Lorenz EN. Deterministic nonperiodic flow. J Atmos Sci 1963;20:130–41.
[2] Bulsara A, Jacobs E, Schieve W. Noise effects in a nonlinear dynamic system: the RF superconducting quantum interference device. Phys Rev A 1990;42:4614.
[3] Wang Z, Wang L, Yin Z-Y, Xia C-Y. Inferring reputation promotes the evolution of cooperation in spatial social dilemma games. PLoS ONE 2012;7:e40218.
[4] Wang Z, Perc M. Aspiring to the fittest and promotion of cooperation in the prisoner's dilemma game. Phys Rev E 2010;82:021115.
[5] Frey M, Simiu E. Noise-induced chaos and phase space flux. Physica D 1993;63:321–40.
[6] Simiu E. Chaotic transitions in deterministic and stochastic dynamical systems: applications of Melnikov processes in engineering, physics, and neuroscience. Princeton University Press; 2002.
[7] Lin H, Yim S. Analysis of a nonlinear system exhibiting chaotic, noisy chaotic, and random behaviors. J Appl Mech 1996;63:509–16.
[8] Yang X, Xu W, Sun Z, Fang T. Effect of bounded noise on chaotic motion of a triple-well potential system. Chaos Solitons Fract 2005;25:415–24.
[9] Liu W, Zhu W, Huang Z. Effect of bounded noise on chaotic motion of duffing oscillator under parametric excitation. Chaos Solitons Fract 2001;12:527–37.
[10] Gan C, Wang Y, Yang S, Lei H. Noisy chaos in a quasi-integrable Hamiltonian system with two DOF under harmonic and bounded noise excitations. Int J Bifurcation Chaos 2012;22.
[11] Fiasconaro A, Spagnolo B, Boccaletti S. Signatures of noise-enhanced stability in metastable states. Phys Rev E 2005;72:061110.
[12] Fiasconaro A, Spagnolo B. Stability measures in metastable states with Gaussian colored noise. Phys Rev E 2009;80:041110.
[13] Wiggins S, Holmes P. Homoclinic orbits in slowly varying oscillators. SIAM J Math Anal 1987;18:612–29.
[14] Wiggins S, Shaw SW. Chaos and three-dimensional horseshoes in slowly varying oscillators. J Appl Mech 1988;55:959–68.
[15] Simiu E. Melnikov process for stochastically perturbed, slowly varying oscillators: application to a model of wind-driven coastal currents. J Appl Mech 1996;63:429–35.
[16] Holmes P, Moon F. Strange attractors and chaos in nonlinear mechanics. J Appl Mech 1983;50:1021–32.
[17] Wiggins S. Global bifurcations and chaos. Springer; 1988.
[18] Wolf A, Swift JB, Swinney HL, Vastano JA. Determining Lyapunov exponents from a time series. Physica D 1985;16:285–317.
[19] Eckmann J-P, Ruelle D. Ergodic theory of chaos and strange attractors. Rev Mod Phys 1985;57:617.
[20] Hsu C. A theory of cell-to-cell mapping dynamical systems. J Appl Mech 1980;47:931–9.
[21] Hsu C. A generalized theory of cell-to-cell mapping for nonlinear dynamical systems. J Appl Mech 1981;48:634–42.
[22] Hsu CS. Cell-to-cell mapping: a method of global analysis for nonlinear systems. New York: Springer; 1987.